

Photon Engine Modeling Using Space 3D TSS™ V12.01

By Joseph M. Clay, Spacedesign

Abstract

Described herein is an engine design for converting radiation pressure conveyed by a light beam(s) into mechanical work (the “Photon Engine”). The Photon Engine employs a novel thermal control technique that entails red-shifting a light beam to reduce residual heat. Fundamental to the red-shifting technique is the utilization of a near total reflective surface(s) (NTRS) and multiple resonating piezoelectric actuators. Operation of the Photon Engine also involves other critical sub-processes, including light beam collection, light beam intensification, and light beam containment. These sub-processes and the physical components responsible for carrying out these sub-processes are described in detail. More generally, the Photon Engine according to this invention operates to convert radiation pressure into electric current via mechanical work. In a preferred mode, the mechanical work is transferred through the NTRSs to resonating piezoelectric actuators in series.

Space 3D TSS™ V12.01 can model the process and apparatus of a photon engine with time dependent ray-tracing, (*i.e.*, temporal ray-tracing). The five temporal ray-tracing capabilities are: (1) force accumulation from radiation pressure exerted by reflections, (2) light containment by variable optical properties as a function of time/ray distance, (3) flux change when switching between enclosures, (4) loss of energy due to red-shift caused by movable mirrors and (5) energy absorption within participating media.

Introduction

A method for collecting, intensifying, and containing light and converting radiation pressure in a light beam into electricity, is presented. Also presented is a photon engine capable of implementing each of these sub-processes, and thereby, converting radiation pressure conveyed by the light beam into useable energy. To harness radiation pressure provided in the light beam, a contained light beam is directed through multiple reflections utilizing a near total reflective surface(s). A near total reflective surface (NTRS) utilizes total internal reflection to eliminate losses from repeated reflections, although participating media causes energy absorption, and is an effective mirror surface that outperforms commercially available mirrors. Conversion of radiation pressure to electricity is achieved through a movable prism having the desired reflective surfaces and piezoelectric actuators operably associated with the movable prism. This method is chosen to achieve a high velocity surface to red-shift the contained light dissipating the residual heat. Light containment is achieved through a compression boundary light switch (CBLS) or surface that changes from totally reflective to totally transparent, nearly instantaneously. A light multiplier is provided for intensifying a collected light beam and also for synchronizing the light collection and light intensification stages of engine operation, with the light containment and light conversion stages.

Space 3D TSS can model the complex multidisciplinary interactions of a collected and contained light beam that is converted to mechanical work. The software models (1) variable optics to model containment using light switching, (2) enclosures to

model flux delta from beam splitting, (3) loss of energy due to red-shift (4) energy absorption within participating media, and (5) force accumulation from radiation pressure exerted by reflections.

Engine Components and Stages of Operation

The photon engine and its operation may be described in terms of four major components or stages of operation: (1) light collector/collection; (2) light intensifier/intensification; (3) light converter/conversion; and (4) electric generator/generation. Figure 1 is a simplified diagram representing these components of the photon engine and stages of operation. Photon engine operation may be understood best by examining the travel of light through the components and the operations performed on the light during this travel.

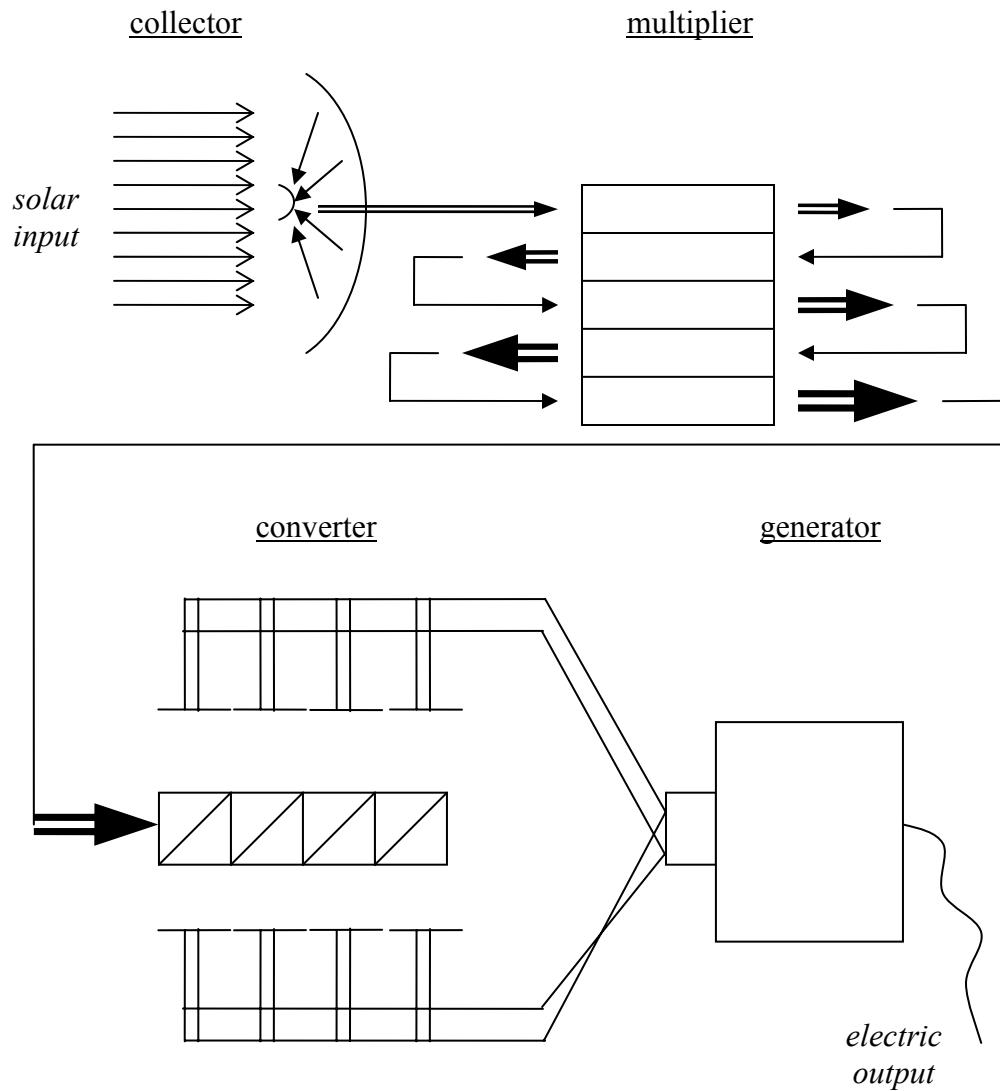


Figure 1 – Exploded view of the four Photon Engine Major Components/Stage

Light Collection

In this first stage, a continuous, concentrated beam is generated from a large area or distribution of collected light. Light is preferably collected from solar input using a large parabolic collector. The beam is focused to a reverse parabolic mirror, wherein the collected light is again collimated into a beam concentrated light. This beam is then directed to the light multiplier. During the intensification stage, this concentrated beam is continuously inputted to the light multiplier.

Intensification

In the intensification stage, the light multiplier receives the concentrated beam from the collector and manipulates the beam to generate a multiplied and intensified beam. This subprocess is performed in synchronization with the other subprocesses and completed prior to introduction of the beam into a containment chamber (of the light converter).

The light multiplier employs both a light expander and a light contractor. The light multiplier wraps the collected light beam around itself, so that the beam, when viewed edge on, appears as ever larger concentric circles (see Figure 2). This process takes a thin beam, with a relative low energy, and increases the beam energy by widening the beam with each concentric circle. The light path continues to make revolutions around the inside of the multiplier, with each forward revolution striking the expander and expanding to the next higher diameter concentric circle. When the beam reaches the outer concentric circle, the light is incident on a mirror surface and reflected in the reverse direction. The light beam then returns in the same path within the light multiplier except in the reverse direction and opposite rotation. When the light beam is incident on the light contractor, the beam diameter is reduced with each reverse revolution. The multiplier generates the most powerful beam when the reverse beam winds back around the multiplier to the initial beam diameter (solid circle). At this point the collected light beam has been converted into a multiplied and thereby, intensified light beam hitting the light switch in both directions.

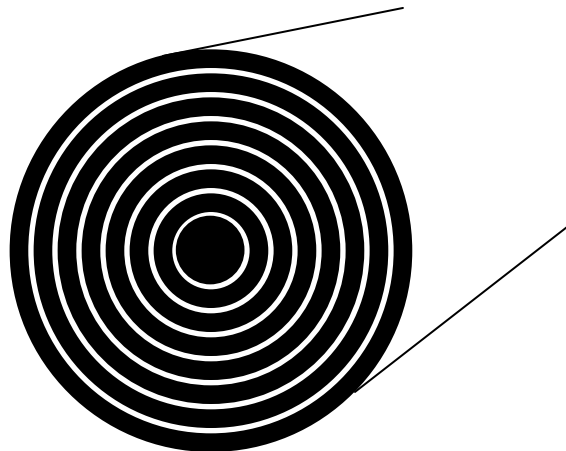


Figure 2 – Multiplied Beam cross-section showing Concentric Circles after 8 rotations in the Light Multiplier.

Conversion

The converter is preferably provided by a containment chamber defined, at least partly, by a prism, including the light switch and two movable prisms. The prisms provide the NTRS and movable, reciprocating mechanisms for the engine.

The light conversion stage is initiated by the light switch going from totally reflective to totally transparent (open mode). With the switch open, the intensified light beam is injected into a containment chamber. When the light multiplier is completely empty, the light switch is returned to totally reflective (closed mode) (which again initiates the intensification subprocess). The contained beam is directed incident on two NTRSs (see Figure 3), and the switch (which is in close mode). This contains light and causes continuous reflections until energy is depleted. The reflections are incident on the NTRSs and radiation pressure conveyed by the beam causes a prism(s) embodying the NTRSs to move. The prisms are connected to an effect stacked piezoelectric actuators. In this way, radiation pressure is harnessed and converted into mechanical work (by way of the moving prism and then the contracting piezoelectric actuators). The conversion process is further explained in the science portion of this paper.

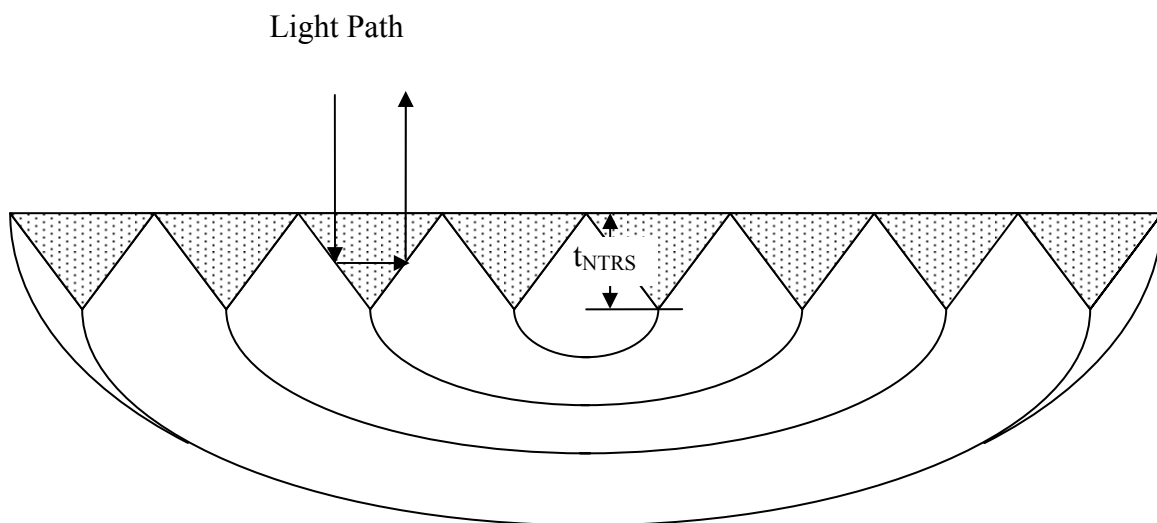


Figure 3 – Cut away view of a Near Total Reflective Surface (NTRS)

Electric Generation

The electric generation stage occurs simultaneously with the light conversion stage. The stacked resonating piezoelectric actuators are attached directly to the NTRSs. For the duration of the light conversion stage, the actuators contract and provide a necessary thermal control benefit of red-shifting the contained light by moving the NTRS faces away from the incident beam at a high velocity. The additional electric current from the force applied by the light through the NTRSs to the piezoelectric actuators is then collected using an H-Bridge (or similar) circuit.

There are some additional design and manufacturing considerations. Figure 4 depicts an inlet to the light multiplier. Notice that the incident beam is normal to the extended tab avoiding Brewster's angle which would cause reflections [1]. Hence the machine is designed to have all incident beams strike quartz along the surfaces normal. This also prevents dispersion, or wave length dependent refraction, which would cause the light to disperse based on wavelength (rainbow effect). Light that is incident along a surface normal will cause specular reflection. Within the containment chamber this is acceptable because the light is still reflected.

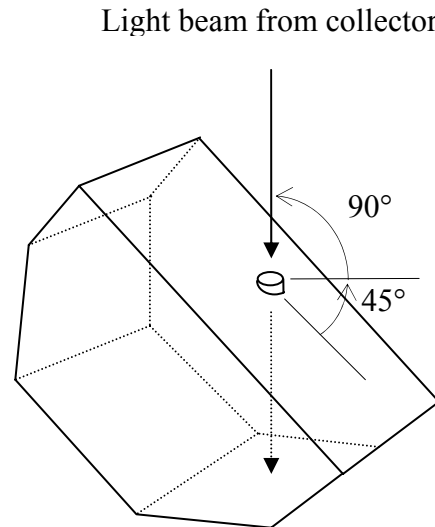


Figure 4 – Entrance of collected light beam into Light Multiplier

Science Behind the Photon Engine

The science behind the design of the Photon Engine may be described by the following equations: a governing work equation; Fresnel equations applied to light switching; a simplistic extinction equation to quantify light as it moves through a region of participating media; and Snell's Law to describe total internal reflection. The governing work equation provides a single equation for calculating the work output of a photon engine. The Fresnel equations show light switching using beyond critical angle tunneling of evanescent waves and can be applied in designing the required switching mechanism for containing light. The participating media provides a measure of light absorption within the quartz. Multiple components of the photon engine rely on the transport of energy through quartz. Snell's law describes light refraction and also when the resulting refraction angle becomes imaginary, that light is totally internally reflected (TIR).

Work Equation for a Photon Engine

The mechanical work generated, W , by the engine can be described by the work equation of a piston-mass system [2] that relates momentum transfer, or radiation pressure, between the light beam and a movable mirror surface. The following equation includes an initial velocity of the movable mirrors and shows light beam red-shift is cancelled by light beam lengthening (see Appendix 1 – Derivation of a Work Equation for a Photon Engine).

$$W = \frac{1}{2} m \left(\left(\frac{p_0 A_m t_0}{m} \left(\frac{1 - (\rho_m \tau_s)^z}{1 - \rho_m \tau_s} \right) + v_0 \right)^2 - v_0^2 \right) \quad (1)$$

where

p_0	is initial radiation pressure,
A_m	is area of each mirror,
t_0	is time duration of initial beam strike,
m	is mass of mirror/piston assembly,
ρ_m	is effective reflectance of mirrors,
τ_s	is effective transmission of light switch,
z	is number of allowed bounces during momentum transfer, and
v_0	is initial velocity of the mirrors.

The efficiency of the engine can be calculated by dividing the work, shown in (1), by the total energy contained in the initial light beam.

Light Switching using beyond Critical Angle Tunneling of Evanescent Waves

Containing light requires a mechanism to rapidly switch from total reflection to total transmission. One embodiment of this light switch, referred to as a compression boundary light switch (CBLS), employs two quartz prisms that are positioned adjacent one another, as shown in Figure 5. The quartz prisms are separated by a small distance, d . Initially, the separation is set at a significantly large, d_r , so as to produce total internal reflection, (see Figure 5(A)). When the two prisms are brought very close together, so that only a very small distance, d_t , separate the prisms, the light is totally transmitted, see Figure 5 (C). In the interim, while the surfaces are moving together the light senses the other surface and the light is both transmitted and reflected, see Figure 5 (B). The amount of transmission can be solved as a multiple boundary problem using Fresnel equations [3].

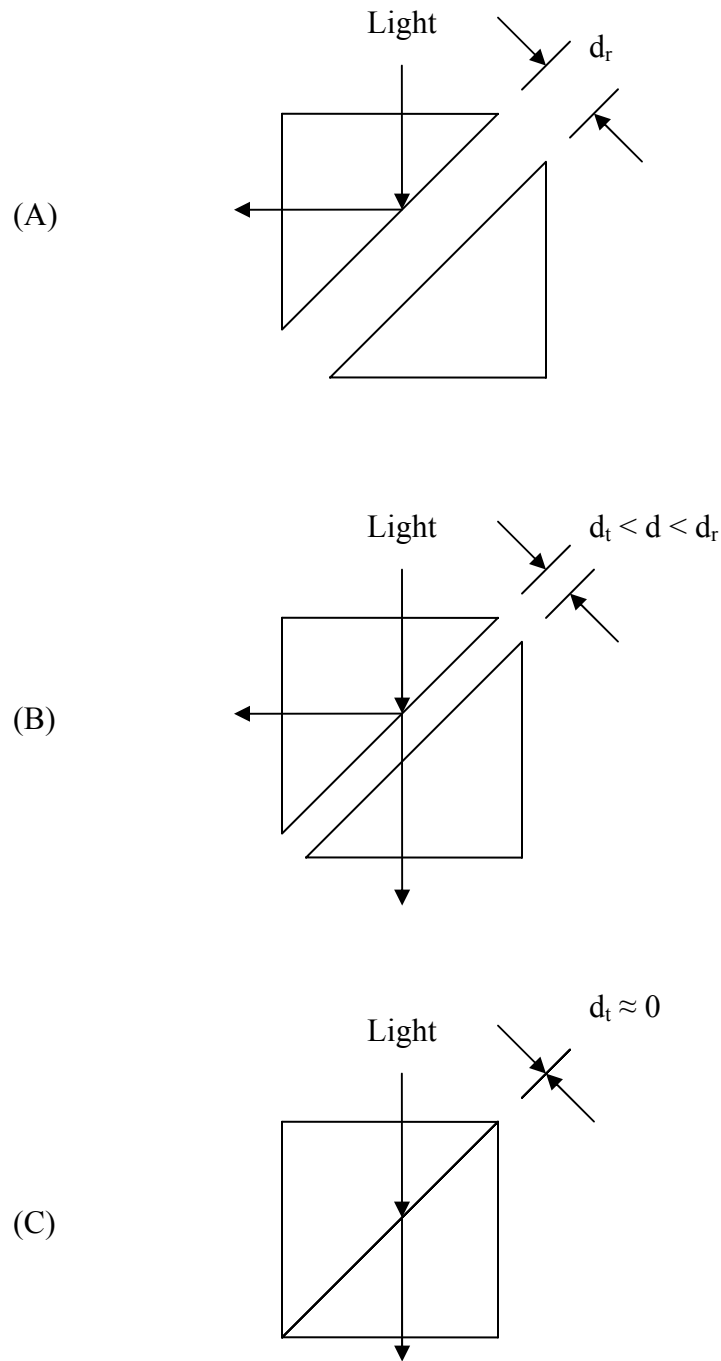


Figure 5 – Stages of Light Switching using Beyond Critical Angle Tunneling of Evanescent Waves: (A) Total Reflection, (B) Transition from Total Reflection to Total Transmission, and (C) Total Transmission.

When the separation between the two quartz prisms is sufficiently narrow, an evanescent wave stimulates the second surface so that light is transmitted. The amount of transmission is a function of the incident angle, gap index of refraction, quartz prism index of refraction, light wavelength and the polarization of the light.

The total transmission for p-polarization is shown (2).

$$T_p^{tot} = \frac{n_t \cos \theta_t}{n_i \cos \theta_i} \frac{|t_p^{i \rightarrow m}|^2 |t_p^{m \rightarrow t}|^2}{|e^{-ik_m d \cos \theta_m} - r_p^{m \rightarrow i} r_p^{m \rightarrow t} e^{ik_m d \cos \theta_m}|^2} \quad (2)$$

The total transmission for s-polarization is shown (3).

$$T_s^{tot} = \frac{n_t \cos \theta_t}{n_i \cos \theta_i} \frac{|t_s^{i \rightarrow m}|^2 |t_s^{m \rightarrow t}|^2}{|e^{-ik_m d \cos \theta_m} - r_s^{m \rightarrow i} r_s^{m \rightarrow t} e^{ik_m d \cos \theta_m}|^2} \quad (3)$$

Fresnel coefficients t_p , t_s , r_p and r_s are direct consequences of Maxwell's equations. The coefficients are shown for p-polarization in (4.1-4.4).

$$t_p^{i \rightarrow m} = \frac{2 \cos \theta_i \sin \theta_m}{\cos \theta_m \sin \theta_m + \cos \theta_i \sin \theta_i} \quad (4.1)$$

$$t_p^{m \rightarrow t} = \frac{2 \cos \theta_m \sin \theta_t}{\cos \theta_t \sin \theta_t + \cos \theta_m \sin \theta_m} \quad (4.2)$$

$$r_p^{m \rightarrow i} = -\frac{\cos \theta_m \sin \theta_m - \cos \theta_i \sin \theta_i}{\cos \theta_m \sin \theta_m + \cos \theta_i \sin \theta_i} \quad (4.3)$$

$$r_p^{m \rightarrow t} = -\frac{\cos \theta_t \sin \theta_t - \cos \theta_m \sin \theta_m}{\cos \theta_t \sin \theta_t + \cos \theta_m \sin \theta_m} \quad (4.4)$$

The coefficients are shown for s-polarization in (5.1-5.4).

$$t_s^{i \rightarrow m} = \frac{2 \cos \theta_m \sin \theta_i}{\cos \theta_i \sin \theta_m + \cos \theta_m \sin \theta_i} \quad (5.1)$$

$$t_s^{m \rightarrow t} = \frac{2 \cos \theta_t \sin \theta_m}{\cos \theta_m \sin \theta_t + \cos \theta_t \sin \theta_m} \quad (5.2)$$

$$r_s^{m \rightarrow i} = -\frac{\cos \theta_i \sin \theta_m - \cos \theta_m \sin \theta_i}{\cos \theta_m \sin \theta_i + \cos \theta_m \sin \theta_i} \quad (5.3)$$

$$r_s^{m \rightarrow t} = -\frac{\cos \theta_m \sin \theta_t - \cos \theta_t \sin \theta_m}{\cos \theta_m \sin \theta_t + \cos \theta_t \sin \theta_m} \quad (5.4)$$

Total p-polarized transmission is solved as function of gap distance and wavelength (6) and the results are plotted on the graph of Figure 6.

$$T_p^{tot} = \frac{3.686}{e^{4.443 \frac{d}{\lambda}} + e^{-4.443 \frac{d}{\lambda}} + 1.686} \quad (6)$$

Total s-polarized transmission is solved as function of gap distance and wavelength (7) and the results are plotted on the graph of Figure 7.

$$T_s^{tot} = \frac{1.437}{e^{4.443 \frac{d}{\lambda}} - e^{-4.443 \frac{d}{\lambda}} - 0.5604} \quad (7)$$

The total transmission and total reflection states occur at $d_t = 0$ nm and $d_r > 1000$ nm, respectively, for the visible spectrum of light (400 nm – 700 nm). This provides a minimum operating criterion for a CBLS and indicates that the total transmission state, without perfectly flat surfaces, requires that the quartz prisms be compressed together.

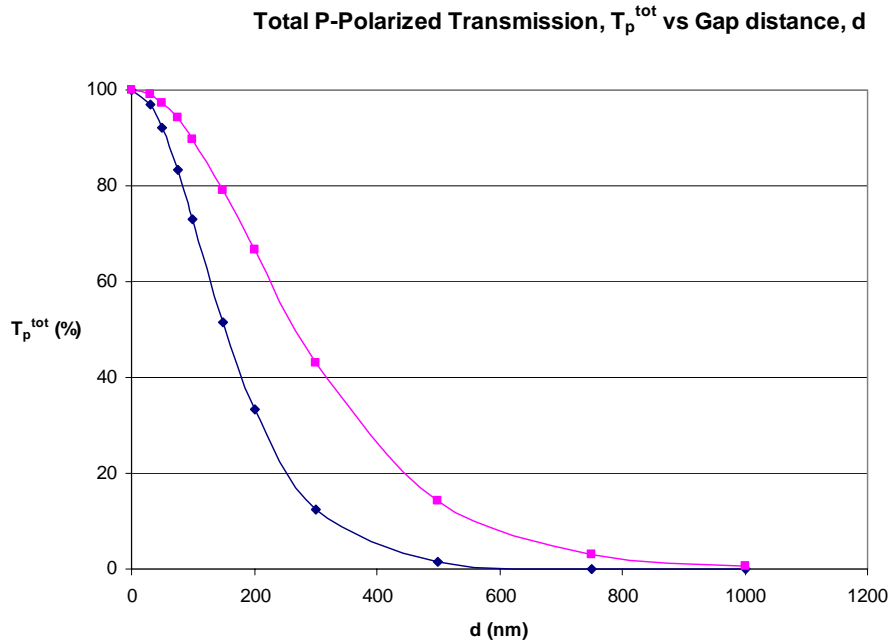


Figure 6 – Total P-Polarized Transmission vs. Gap Distance

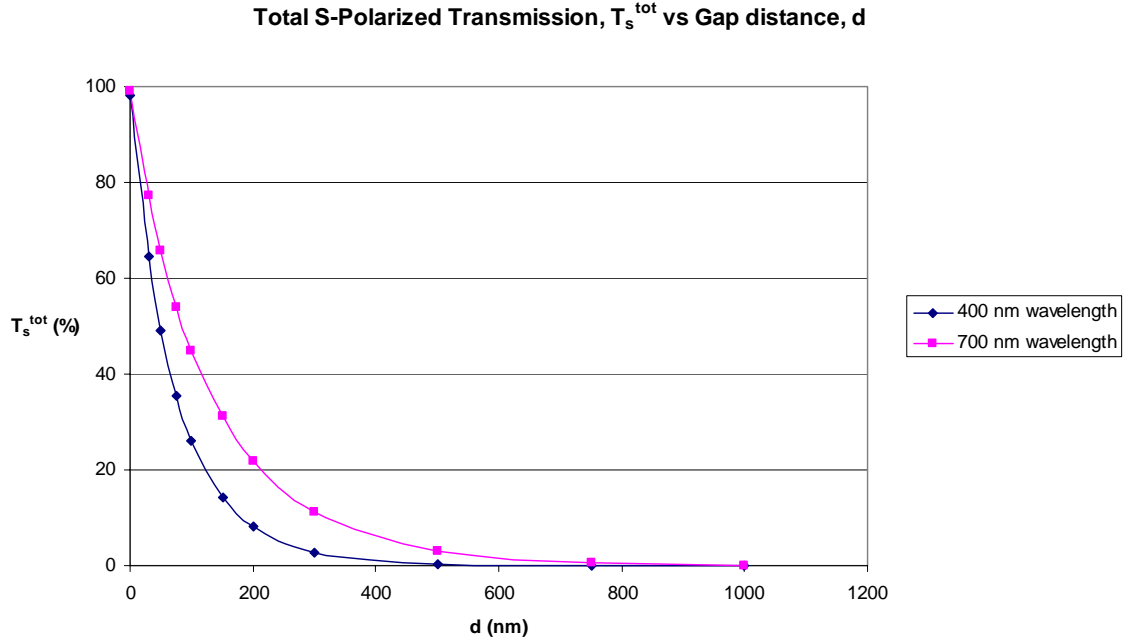


Figure 7 – Total S-Polarized Transmission vs. Gap Distance

Red-shift, Total Internal Reflection (Snell's Law), and Participating Media

A near total reflective surface (NTRS) uses total internal reflection to eliminate losses from repeated reflections. Although participating media causes energy absorption and red-shift causes energy dissipation, the NTRS provides an effective mirror surface that outperforms commercially available mirrors.

Referring to Figure 8, an initial energy packet, dQ_{INITIAL} , is incident on a surface with a velocity, v , moving directly away. The velocity vector is directly aligned with this initial energy packet direction vector. The resulting incident energy, dQ_{INCIDENT} , is reduced by red-shift, a function of the speed of light, c as (8).

$$dQ_{\text{INCIDENT}} = dQ_{\text{INITIAL}} \left(\frac{c - v}{c} \right) \quad (8)$$

Snell's law [1] describes light refraction so that when the resulting refraction angle becomes imaginary the light is totally internally reflected. The reflected energy, dQ_{REFLECT} , is equal to the incident energy as (9)

$$dQ_{\text{REFLECT}} = dQ_{\text{INCIDENT}} \quad (9)$$

Since the reflected energy contacts the other side of the prism at a right angle to the velocity vector there is no red-shift, hence dQ_{FINAL} , is equal to the reflected energy as (10)

$$dQ_{\text{REFLECT}} = dQ_{\text{FINAL}} \quad (10)$$

Although the incident energy is less with a higher velocity, the resulting force is nearly the same. The work output from two equal forces, one against a lower surface velocity and the other against a higher surface velocity is not the same. The higher surface velocity will produce a higher work output, as shown in Eq. (1), because the final velocity (first square term) is referenced from the initial velocity (second square term). If red-shift approaches the reflectivity of the mirror, by moving the mirror surface fast enough, the contained energy will be dissipated through red-shifting lowering the residual heat. This is a unique and innovative thermal control technique.

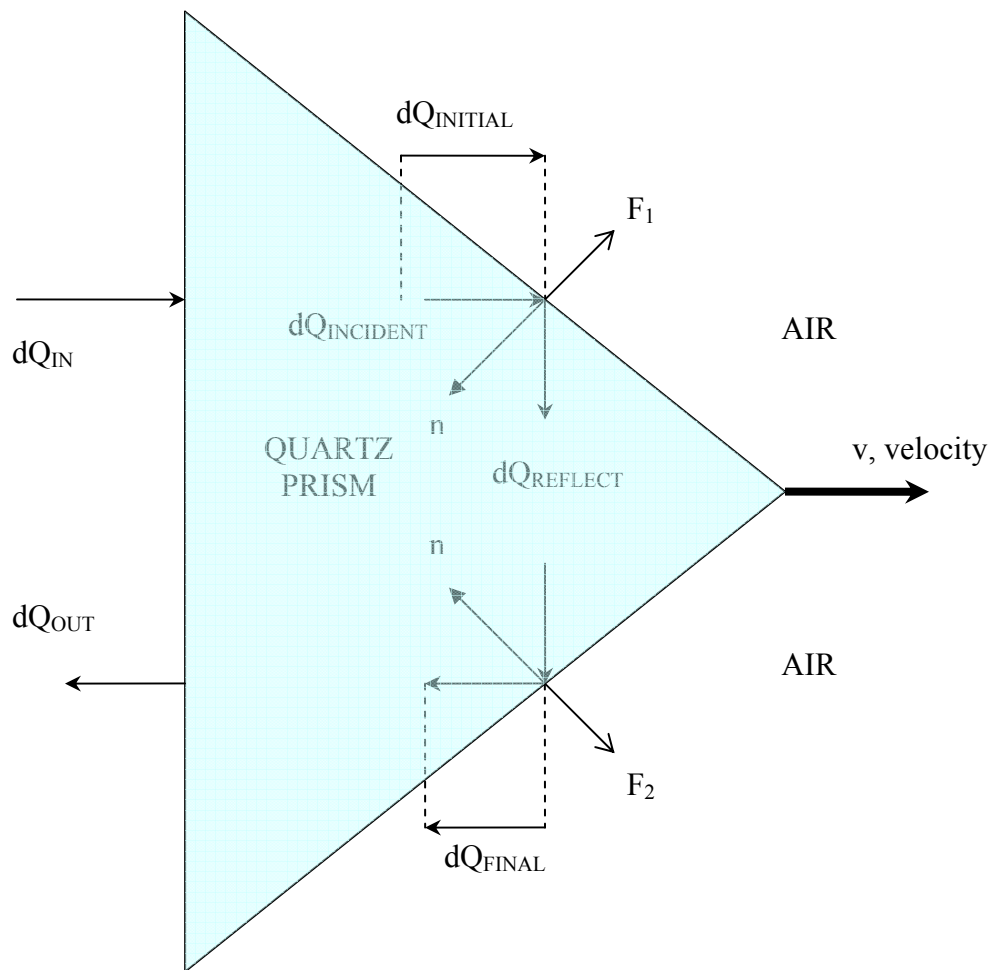


Figure 8 – Total Internal Reflection (Snell’s Law) coupled with Red-shifting inside a Moving Quartz Prism

Stacked piezoelectric actuators in resonance provide a mechanism for efficiently converting mechanical work into electricity, while obtaining a high NTRS velocity for red-shifting [4].

Participating media effects radiation exchange through a volume. The media (or medium) through which the radiation travels can cause attenuation. For simple materials, such as a gas at radiative equilibrium, the dependence on wavelength can be ignored.

This is also possible for solids such as quartz. This simplification allows the use of a simple absorption coefficient [5].

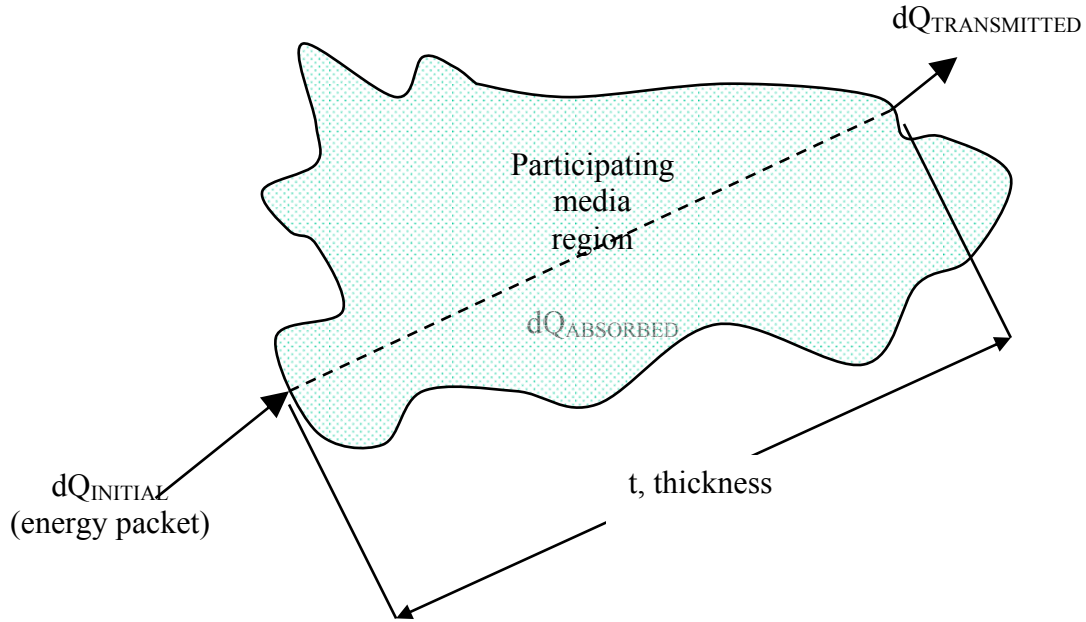


Figure 9 – Energy Absorption within a Participating Media Region

The initial energy packet, $dQ_{INITIAL}$, enters the region where it can interact, or refract as shown, where it encounters the participating media. As the energy packet travels through the participating media it loses media as that is absorbed, $dQ_{ABSORBED}$, by the media. As the energy packet exits the media, the transmitted energy, $dQ_{TRANSMITTED}$, can again interact, or refract as shown, with the participating media.

An energy balance can be written for the energy packets as (11).

$$dQ_{INITIAL} = dQ_{ABSORBED} + dQ_{TRANSMITTED} \quad (11)$$

The transmitted energy left after absorption is calculated using the absorption coefficient as (12)

$$dQ_{TRANSMITTED} = dQ_{INITIAL} e^{-at} \quad (12)$$

The absorbed energy can be calculated as (13)

$$dQ_{ABSORBED} = dQ_{INITIAL} (1 - e^{-at}) \quad (13)$$

The NTRS effective reflectance, ρ_{NTRS} , can be calculated as (14)

$$\rho_{NTRS} = \frac{dQ_{OUT}}{dQ_{IN}} = \rho_{QUARTZ} + (1 - \rho_{QUARTZ}) e^{-at_{total}} \left(\frac{c - \nu}{c} \right) \quad (14)$$

Note that scattering is assumed to be negligible and negative absorption is not considered in this case [5]. The quartz surface specular reflectance, ρ_{QUARTZ} , is also included.

Simulation Modeling using Space 3D™ TSS

The science behind the Photon Engine is now modeled using the Space 3D Thermal software package. This collection of enhancements facilitate temporal ray tracing. The five temporal ray tracing capabilities are:

- (1) force accumulation from radiation pressure exerted by reflections.
- (2) variable optics to model containment using light switching,
- (3) enclosures to model flux delta from beam multiplying and splitting,
- (4) loss of energy from redshift,
- (5) energy absorption within participating media,

The first capability expands the calculation of radiation pressure (or radiation force) to include forces from reflected energy. Previous versions of TSS (i.e. V10.01 and V11.01) included radiation pressure from only a direct heating component to a node. Radiation pressure from reflected energy is the most fundamental concept of modeling an operational photon engine by modeling internal momentum transfer from photons to a movable piston during multiple reflections.

The second capability is light containment by time varying optical properties. This capability is required to extend the simulation of a photon engine to include multiplication of a light beam. This is accomplished by modeling a surface that begins as highly reflective, then after a finite amount of time instantly changing the optical properties to allow transmission. After a subsequent finite amount of time, the surface is instantly changed back to highly reflective. Unlike the first case capability, having time dependent properties allows for the multiplication of the beam power as shown in the third case.

The third capability is flux change when switching between enclosures. This capability calculates the flux change in a source (or flux delta) when a long lower flux beam is wrapped around itself then split by variable optics switch to produce a shorter higher flux beam. This process effectively compresses the beam length, and since the total energy remains the same, the result is a higher flux beam.

Figure 10 and 11 show a continuum view of temporal ray-tracing and Flat land (i.e. timesheet) view of temporal ray-tracing.

Temporal ray-tracing continuum diagram

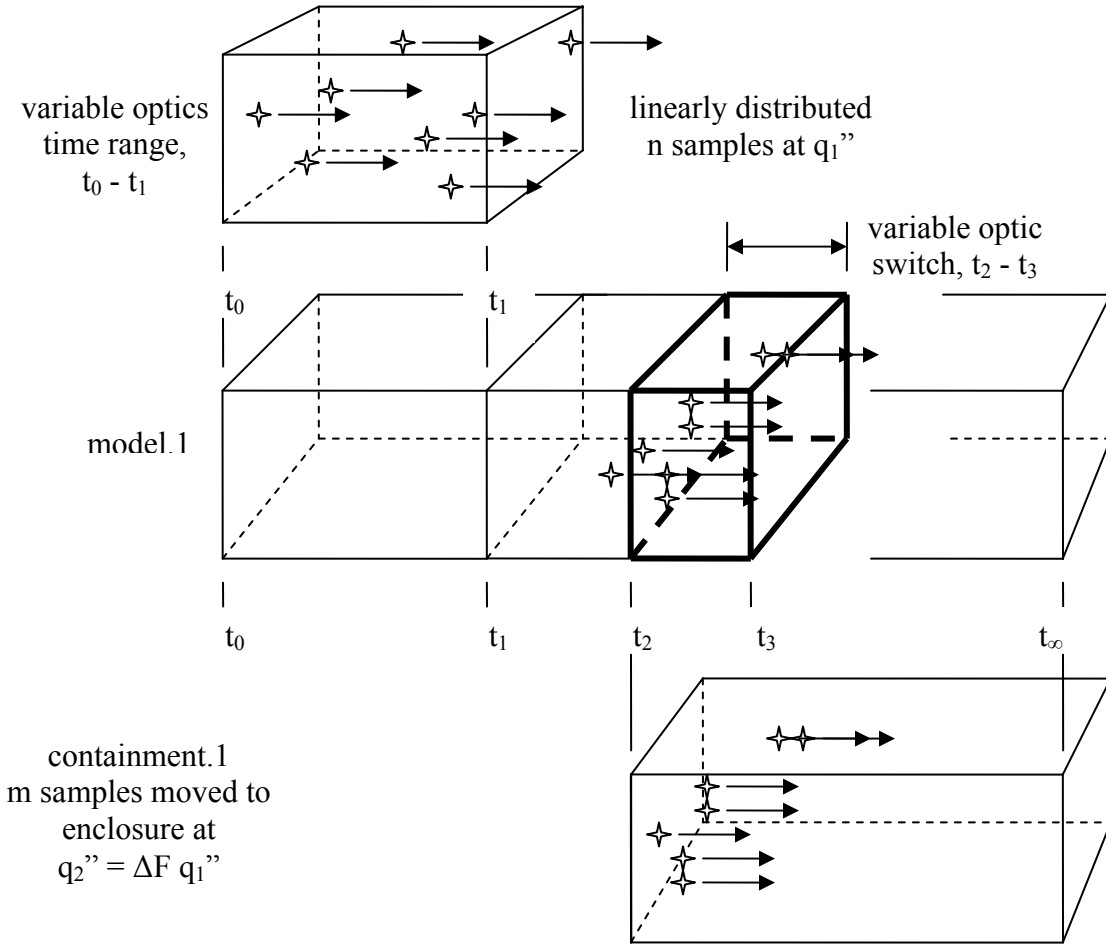


Figure 10 – Temporal ray-tracing timesheet diagram showing model.1 and containment.1

Temporal ray-tracing Flat land diagram

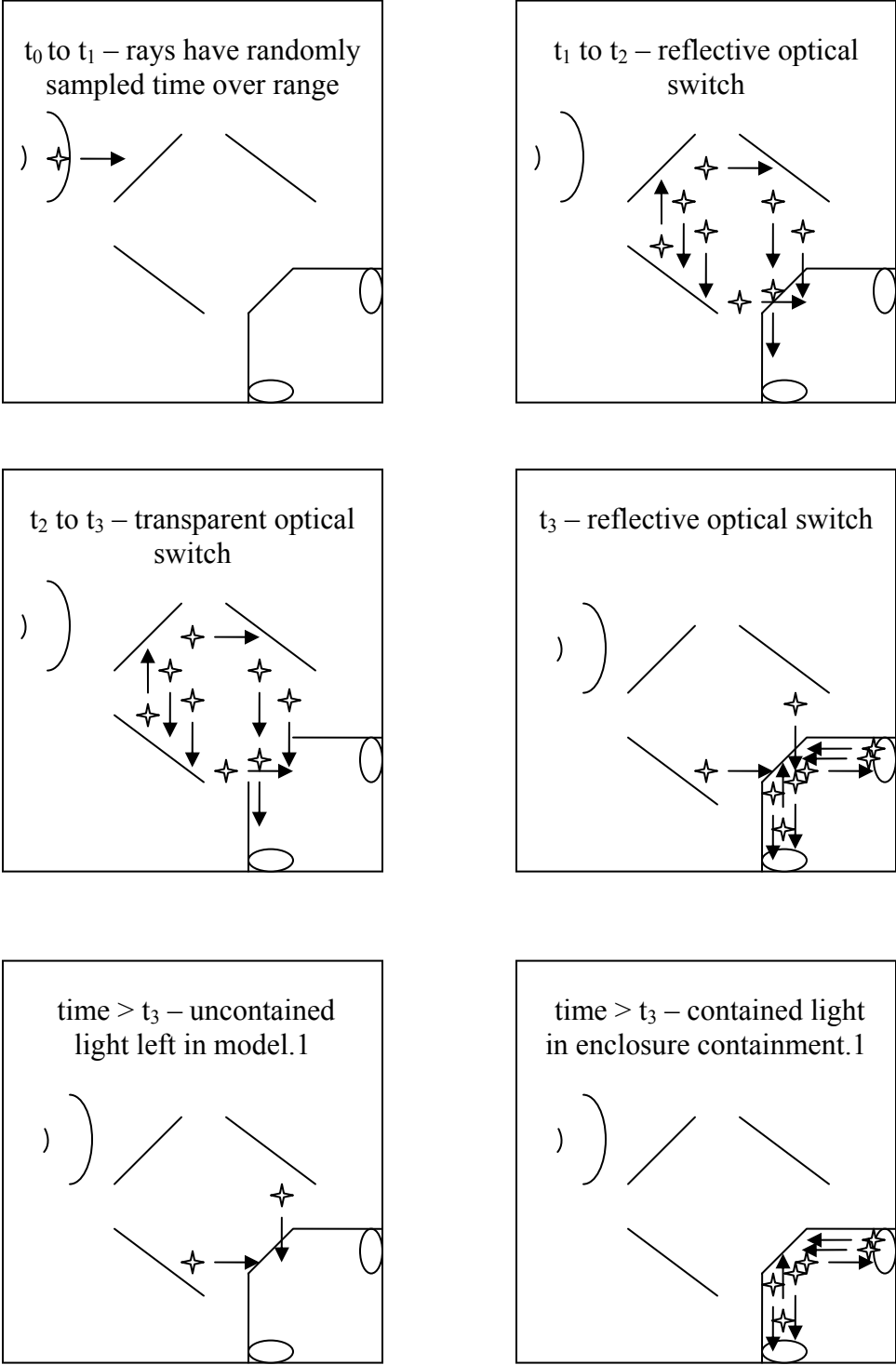


Figure 11 – Temporal Flat land time sheets with variable optics switching

The flux delta, ΔF , is calculated by taking into account the number of sample rays, n , the number of contained rays, m , and the different sample times, initial sample range, t_0 to t_1 , and variable optics switch range, t_2 to t_3 as (15)

$$\Delta F = \frac{m (t_1 - t_0)}{n (t_3 - t_2)} \quad (15)$$

The flux delta can be used to determine the containment chamber flux, q''_2 , of the multiplied beam from the model.1 flux, q''_1 , as (16)

$$q''_2 = \Delta F q''_1 \quad (16)$$

The fourth capability is the loss of energy in beam strength due to red shift. In a machine with momentum transfer to a movable piston, the movement of the piston away from the incident beam will cause red shifting of the reflected energy. This can be modeled by simply reducing the reflected ray energy based on the velocity the surface moves during the reflection.

The fifth capability is the loss of energy from absorption by participating media. This phenomenon occurs when light is transmitted through a solid such as quartz. The light path inside a photon engine requires many interactions with quartz. The interaction inside the light multiplier will result in rays traveling long distances inside quartz. The longer a ray travels inside quartz the more energy lost to absorption. This results in lower transmission and heating of the participating media. The most desirable operation of a photon engine is to have the lowest absorption (highest transmission) so the energy is available for momentum transfer.

Figure 12 shows a control volume approach for participating media.

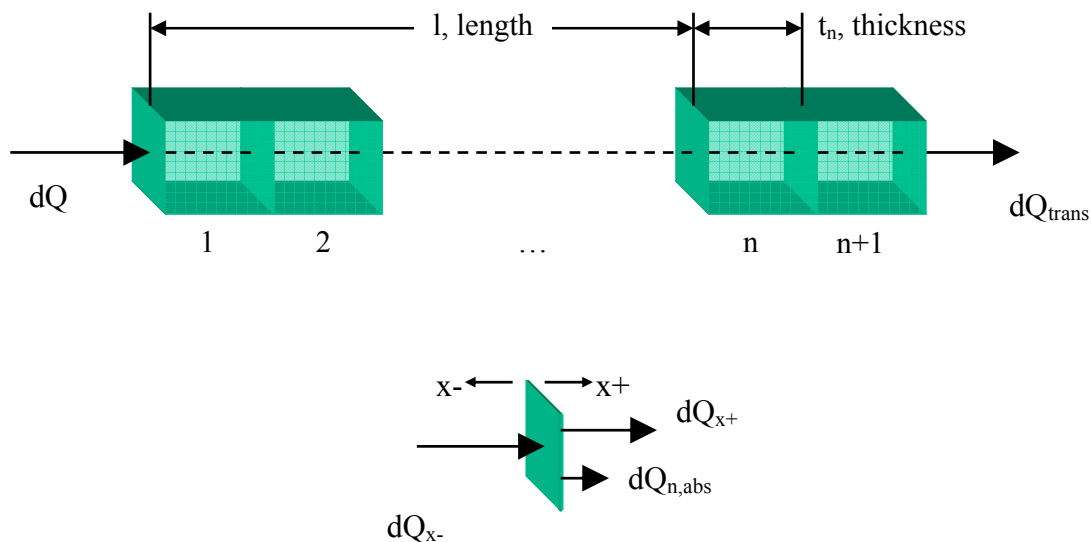


Figure 12 – Control Volume representation for Participating Media Region

Instead of representing the participating media region as a continuous volume, meshing the region into smaller control volumes allows the absorption to be quantified

discretely as it moves through a region. As shown in Figure 10, an energy balance on the interface between two control volumes provides the internal heating, $dQ_{n,abs}$, and the energy entering the subsequent control volume, dQ_{x+} , as (17.1-17.2)

$$dQ_{x-} = dQ_{x+} + dQ_{n,abs} \quad (17.1)$$

$$dQ_{n,abs} = dQ_{x+} (e^{-\alpha(l+t_n)} - e^{-\alpha l}) \quad (17.2)$$

Results

An analysis was performed combining all the temporal ray tracing capabilities into a single simulation that accurately simulates a working PE. Care must be taken to avoid aberrations when modeling light as a ray. This distortion occurs when light is focused to a point. The engine design has avoided aberrations. Brewster's angle is also avoided by always totally internally reflecting and transitioning from one media to another along a surfaces normal without any angle of incidence. Figure 13 shows the ray paths for a working PE.

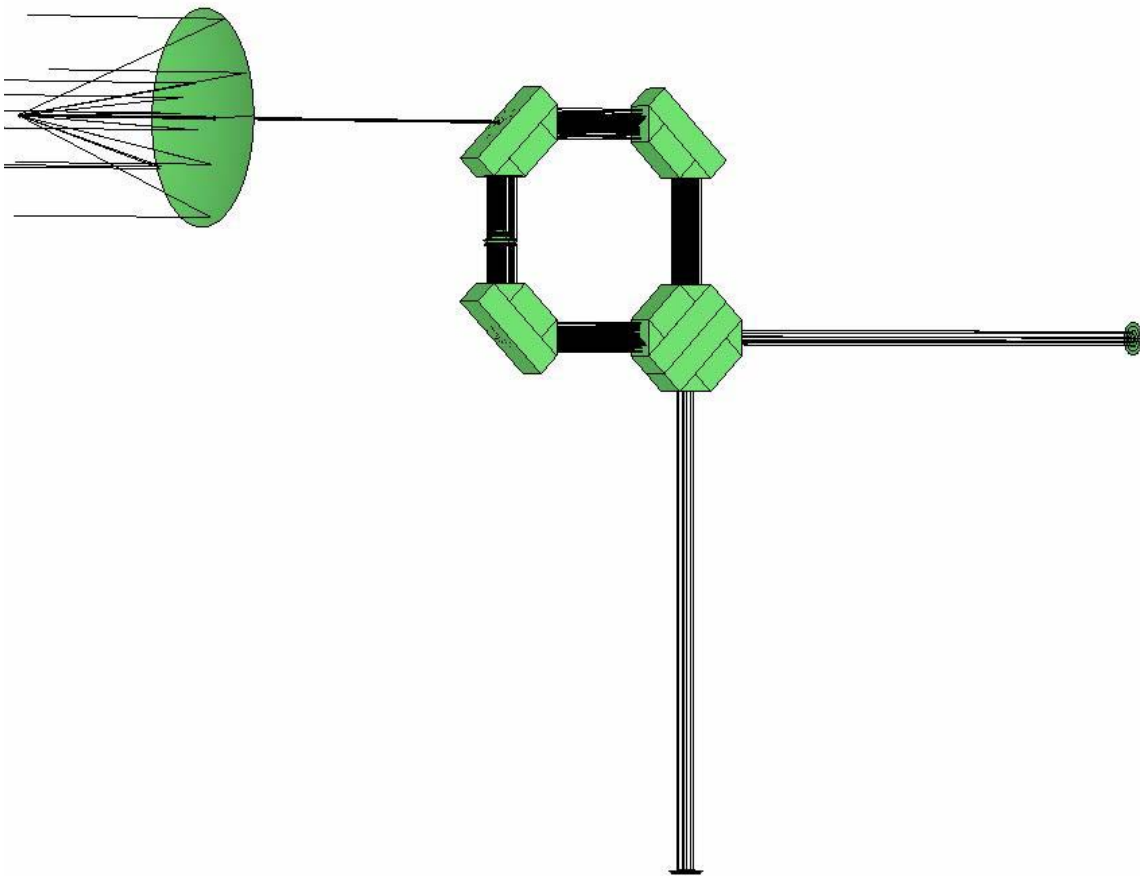


Figure 13 – Working Photon Engine showing ray paths for (1) collection, (2) multiplication, and (3) conversion (note: original CBLS design).

The simulation tool was used to synthesize the design by augmenting the CBLS to have a linear triangular prism design (Linear Switch) that is similar to the NTRS design.

Additional views of the PE components, including the Linear Switch, can be found in Appendix 2.

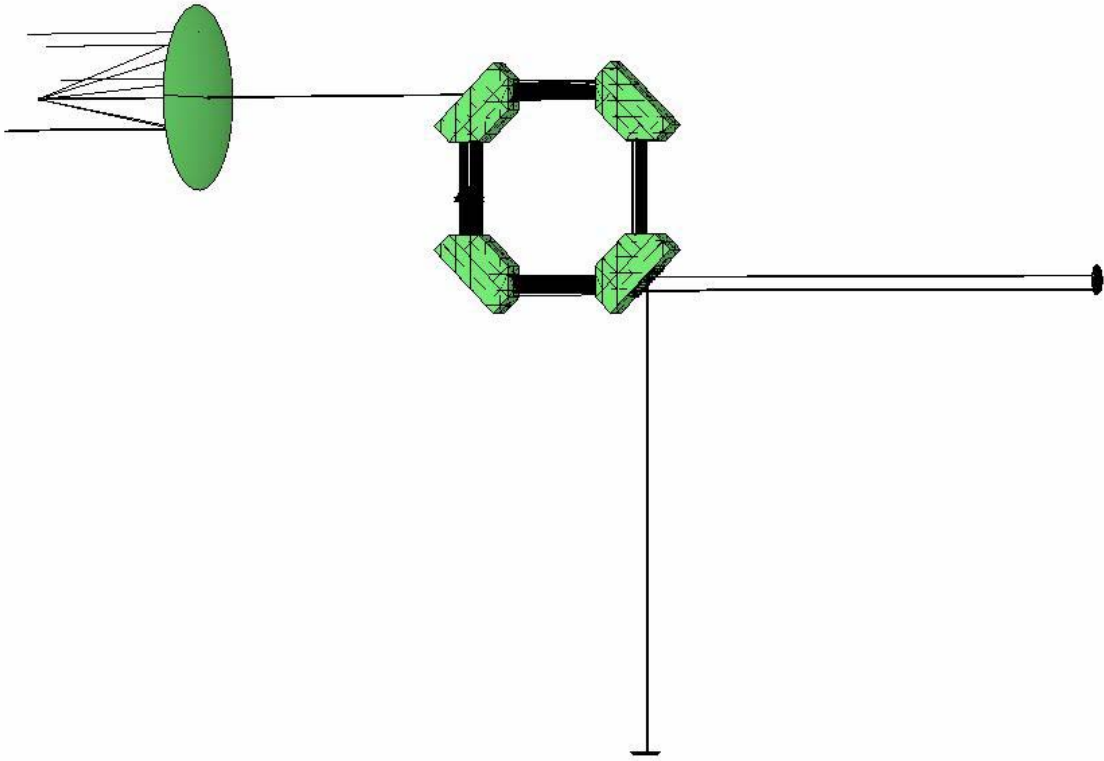


Figure 14 – Working Photon Engine showing ray paths for (1) collection, (2) multiplication, and (3) conversion (note: linear switch design).

Using a spreadsheet the efficiency of each design has been estimated using the number of reflections inside the containment chamber per ray, estimate of ρ_{NTRS} and τ_{SWITCH} , and lowest available quartz absorption coefficient, α . The NTRS velocity used for the ray tracing was 500 m/s.

Table 1 – Efficiency results for two Photon Engine optical switch designs.

	# of bounces per ray, z	ρ_{NTRS}	τ_{SWITCH}	α -QUARTZ (cm ⁻¹)	Efficiency (%)
Standard CBL Switch	10469	0.99999	0.9999	1 x 10 ⁻⁵	2.07
Linear Switch	136534	0.99999	0.99999	1 x 10 ⁻⁵	15.59

Conclusions

A method and apparatus for collecting, containing, and converting light into electricity has been presented. The engine combines electromagnetism and piezoelectric effect by harnessing radiation pressure and converting that mechanical work directly to electric current. The scientific basis for a governing work equation, light switching using beyond critical angle tunneling of evanescent waves, and red-shifting light within participating media has been shown. Furthermore, a simulation of this method and apparatus, the Photon Engine, has been shown using the Space 3D™ TSS software package. Although the calculated efficiencies are lower than conventional solar panels, further design synthesis could provide further improvements.

Additionally, a thermal control technique has been demonstrated to dissipate residual heat through red-shifting light. The required NTRS surface velocity, or other mirror surface, can be achieved using stacked resonating piezoelectric actuators.

The scientific basis for a governing work equation, light switching using beyond critical angle tunneling of evanescent waves, and red-shifting light within participating media has been shown.

Furthermore, a simulation of this method and apparatus, the Photon Engine, has been shown using the Space 3D™ TSS software package. Although the calculated efficiencies are lower than conventional solar panels, further design synthesis could provide further improvements.

Acknowledgments

The author would like to thank Phillip C. Mackey, Spacedesign, for hours upon hours of programming to develop Space 3D™ TSS V12.01 capabilities, Joseph M. Lepore, Spacedesign, for developing the simulation model, and Alberto Q. Amatong, Jr. for editorial assistance and for legal counsel.

References

1. Smith, T.F., Radiation Heat Transfer Notes, University of Iowa, Department of Mechanical Engineering, Iowa City, IA, 1992
2. Halliday, D. and Resnick, R., Fundamentals of Physics, pp. 852-853, John Wiley & Sons, Inc. New York, NY, 1988
3. Peatross, J. and Stokes, H., Physics of Light and Optics, Brigham Young University, Department of Physics and Astronomy, Provo, UT, 2001
4. Schneider, M. A., Personal Communication, 2005
5. R. Siegel, and Howell, J.R. Thermal Radiation Heat Transfer, 3rd Edition, Hemisphere Publishing Corp., 1992.

Appendix

Appendix 1 – Derivation of Photon Engine Governing Work Equation

Maxwell [2] showed the resulting momentum p is twice the energy, U , divided by the speed of light, c , for a parallel beam of light totally reflected at an angle normal to the incidence.

$$p = \frac{2U}{c} \quad (\text{A-1})$$

This pressure can be multiplied by compressing the beam from its initial length, l_i , to the compressed length, l_c . The multiplied beam has an initial radiation pressure, p_0 , that enters the photon engine containment chamber at time 0 (zero), that is found by the equation.

$$p_0 = \frac{l_i p}{l_c} \quad (\text{A-2})$$

The change in the radiation pressure can be described by the reflectivity (including absorption from participating media), red-shift caused by the movable reflective surface, and the transmission through the light switch.

$$p_1 = \rho_m \tau_s p_0 \frac{c - v_1}{c} \quad (\text{A-3})$$

Generalizing the above equations for arbitrary time n the radiation pressure, p_n , for bounce n is found by the equation.

$$p_n = \rho_m^n \tau_s^n p_0 \left(\left(\frac{c - v_{n-1}}{c} \right) \right) \quad (\text{A-4})$$

The time the beam is incident on the mirror is a function of the red-shift. After each red-shift the beam length increases which increases the incident time.

$$l_1 = l_0 + v_0 t_0 \Rightarrow t_1 = t_0 \frac{c}{c - v_0} \quad (\text{A-5})$$

Generalizing the above equation for arbitrary time n the incident time is shown by the equation.

$$t_n = t_0 \left(\left(\frac{c}{c - v_{n-1}} \right) \right) \quad (\text{A-6})$$

The velocity increase, Δv_n , of the piston head at arbitrary time n is calculated by the equation.

$$\Delta v_n = \frac{\rho_n \tau_n p_{n-1} A_m}{m} t_{n-1} \quad (\text{A-7})$$

The velocity, v_z , at time z is calculated by summing v over the time 0 to z .

$$v_z = \sum_{n=1}^z \Delta v_n + v_0 = \sum_{n=1}^z \frac{\rho_m \tau_s p_{n-1} A_m}{m} t_{n-1} + v_0 \quad (\text{A-8})$$

$$v_z = \frac{\rho_m \tau_s A_m}{m} \sum_{n=1}^z p_{n-1} t_{n-1} + v_0 \quad (\text{A-9})$$

$$v_z = \frac{\rho_m \tau_s A_m}{m} \sum_{n=1}^z \rho_m^n \tau_s^n p_0 \left(\left(\frac{c - v_{n-1}}{c} \right)! \right) t_0 \left(\left(\frac{c}{c - v_{n-1}} \right)! \right) + v_0 \quad (\text{A-10})$$

$$v_z = \frac{\rho_m \tau_s A_m}{m} p_0 t_0 \sum_{n=1}^z \rho_m^n \tau_s^n + v_0 \quad (\text{A-11})$$

The work, W , generated by the photon engine is calculated by the equation.

$$W = \frac{1}{2} m (v_z^2 - v_0^2) \quad (\text{A-12})$$

$$W = \frac{1}{2} m \left(\left(\frac{\rho_m A_m}{m} p_0 t_0 \sum_{n=1}^z \rho_m^n \tau_s^n + v_0 \right)^2 - v_0^2 \right) \quad (\text{A-12})$$

The summation can be re-written using a power series solution. The result is the short form of the governing work equation.

$$W = \frac{1}{2} m \left(\left(\frac{p_0 A_m t_0}{m} \left(\frac{1 - (\rho_m \tau_s)^z}{1 - \rho_m \tau_s} \right) + v_0 \right)^2 - v_0^2 \right) \quad (\text{A-13})$$

Appendix 2 – Various close-up views of Photon Engine components

